

24 **Abstract**

25 Variability and changes in the individual life-history parameters of fishes are frequently
26 overlooked, and it is assumed that all individuals mature, spawn, grow, and die at the
27 same rates over their lifespans. Here, the variability in the individual growth of the
28 rudimentary hermaphrodite *Diplodus annularis* (Linnaeus, 1758) is described using a
29 Bayesian approach. This approach enables the inference of individual growth curves,
30 even in a species of a relatively short lifespan, and revealed a biphasic growth pattern
31 for this species. Conventional von Bertalanffy growth failed to fit the individual back-
32 calculated lengths-at-age data well. A generalization of this model is proposed for
33 accommodating one change in the growth rate at some moment of the lifespan of this
34 species. This novel five-parameter model (L_{∞} , k_0 , k_1 , t_0 and t_1 , i.e., size at infinite age,
35 initial and final growth rate, age at size zero and age at the change of growth rate)
36 represents the different allocation of energy to somatic growth or reproduction, prior to
37 and post sexual maturity. Moreover, between-sex growth differences are described;
38 juvenile fish display similar growth rates in both sexes, but mature females have lower
39 growth rates than males. The detailed description of the growth of the *D. annularis*
40 shown here can provide adequate input for future implementation of population
41 dynamics models that take into account individual variability (e.g., IBMs, individual-
42 based models). These models could facilitate the management of a species targeted by
43 recreational fishery.

44 **Keywords**

45 Back-calculation, Bayesian inference, biphasic growth, *Diplodus annularis*, energy
46 allocation, rudimentary hermaphrodites

47

48

49 **Introduction**

50 Fisheries biologists and managers have traditionally focused the management of
51 exploited stocks by means of models that incorporate growth descriptions as well as
52 other variables such as age and size distributions, survival, reproductive potential and
53 recruitment (e.g., Haddon, 2001). The growth parameters are explicitly incorporated
54 into traditional population dynamics models used for establishing sustainable
55 exploitation levels of fish stocks (Beverton and Holt, 1957).

56 However, the conventional growth models (i.e., a single observation per fish)
57 clearly overlook individual variability because they do not include the individual
58 characteristics of exploited fish. Population growth is usually described through mean
59 growth parameters (known as “average” growth; Pilling et al., 2002). Recently, studies
60 reported the relevance of the variability at within-population level to estimate and
61 improve the population growth (see Troynicov and Walker (1999) using stochastic
62 models). Thus, it is unreasonable to assume that all individuals will have the same
63 growth pattern in a wild population (Sainsbury, 1980; Smith et al., 1997). This
64 procedure introduces a bias when life expectation depends on size, as is the case for
65 most size-selective fisheries (faster growing fishes tend to be younger when fished, both
66 in commercial [Jackson et al., 2001; Watson and Pauly, 2001; Pauly et al., 2003] and
67 recreational fisheries [Cooke and Cowx, 2006; Lewin et al., 2006]).

68 The back-calculation of length-at-age data contained in fish hard parts, such as
69 otolith growth increments, is considered the most realistic method to obtain information
70 prior to capture (Pilling et al., 2002). Fitting the length-at-age data with the aid of
71 Bayesian inference has allowed for estimating the individual von Bertalanffy
72 trajectories and their variability at the population level (Pilling et al., 2002; Helser and
73 Lai, 2004; Helser et al., 2007). However, instead of using the conventional von

74 Bertalanffy model based in three parameters, several authors recently proposed an
75 extension that accommodates for one change of growth rate at some moment of the
76 lifespan to account for the different distribution of the energy for reproduction versus
77 somatic growth along the lifespan (Day and Taylor, 1997; Lester et al., 2004; Charnov,
78 2005; Charnov, 2008; Quince et al., 2008a; Quince et al., 2008b). The growth rate (k)
79 would not be a meaningful parameter if these life-history phases are not considered
80 (Charnov, 2008). Day and Taylor (1997) suggested that the somatic growth trajectory
81 should be specified by two different equations; one for the prior-maturity period (i.e.,
82 the entire energy supply is devoted to somatic growth) and one for the post-maturity
83 period (i.e., most of the energy supply is devoted to reproduction). This growth pattern
84 is known as biphasic somatic growth (Quince et al., 2008a; Quince et al., 2008b).

85 Here, we describe the individual growth of *Diplodus annularis* (Linnaeus, 1958),
86 commonly known as annular seabream. This species is a small Sparid that inhabits the
87 Mediterranean and Black Sea coast, the Atlantic from the gulf of Biscay to Gibraltar,
88 and the Madeira and Canary Islands (Bauchot, 1987). It is a demersal species, common
89 in the bottoms covered by seagrass beds at 0 to 50 m in depth (Bauchot, 1987). It has
90 been catalogued as a rudimentary hermaphrodite (Buxton and Garratt, 1990). The 50%
91 of the female population reach sexual maturity before males (100 mm versus 90 mm;
92 Matic-Skoko et al., 2007). Until now, population growth parameters have been
93 estimated using the conventional population von Bertalanffy curve (Gordoa and Moli,
94 1997; Pajuelo and Lorenzo, 2001; Matic-Skoko et al., 2007). This conventional version
95 of this model does not fit well with the fast growth experienced by juveniles when they
96 are 1 or 2 years old (Gordoa and Moli, 1997).

97 In the Balearic Islands (NW Mediterranean), this species has low commercial
98 interest and is classified as byproduct or bycatch by the artisanal fleet (data from the

99 Department of Fisheries, Balearic Island Government). Due to this historic low
100 commercial interest in this species, no specific management plan for *D. annularis* has
101 been developed anywhere. In contrast, this species is one of the main targets of
102 recreational fishery (Morales-Nin et al., 2005) and it has been recently reported that this
103 species is vulnerable to the impact of some recreational angling activities (Alós et al.,
104 2008).

105 The main goal of this study is to describe the individual growth pattern of *D.*
106 *annularis* and its intra-population and sex-related variability. Information about the
107 growth at an individual level should facilitate future implementation of individual-based
108 models (IBMs) focused on elucidating the effects of recreational fisheries on the
109 population dynamics of this species.

110 **Materials and methods**

111 **Sampling methods and study area**

112 Experimental fishing sessions were conducted at the Cabrera National Park
113 located on the south coast of Mallorca Island (NW Mediterranean, Fig. 1). This site was
114 selected for two main reasons. First, because recreational angling activities are not
115 allowed (sanctuary area since 1991), the abundance of old individuals is higher than in
116 other open-access sites. Old individuals improve the fit of individual growth trajectories
117 (see results). Second, sites displaying the adequate bottom characteristics for *Diplodus*
118 *annularis* (i.e., bottom dominated by *Posidonia oceanica* beds and placed between 10
119 and 20 m deep) are abundant. A total of 423 individuals were caught between March
120 13th and August 31st 2007 in this area. These individuals were sampled twice a month
121 using hook-and-line methods with conventional recreational gear. All individuals were
122 measured (total length in mm). Sagittal otoliths were extracted and gonads were
123 dissected. This sample was used for describing the distribution of age and size of the

124 population and the individual growth pattern, as well as for testing for the existence of
125 sex-related differences.

126 When a strong relationship between otolith length and fish body length exists (as
127 is the case for *D. annularis*, see Results), it is possible to infer the body size of a fish at
128 younger ages from the width of the annual increments recorded in the otoliths (Pilling et
129 al., 2002). After evaluating the strength of the relationship between otolith size and fish
130 size with a additional second sub-sample (see below), we measured the width of both
131 annual increments and the marginal increment (i.e., the last increment) using a
132 photograph of each left otolith. The images were captured using a video camera
133 (LEICA© M165C and Allied vision technologies© Marlin F080B). Typically, opaque
134 and translucent increments are seen alternating outward from the nucleus (i.e., the
135 growth center of the otolith). The succession of one opaque band and one translucent
136 band was considered one annual increment. The x_i, y_i coordinates of the nucleus, the
137 coordinates of all the annual increments along a predefined growth axis, and the
138 coordinates of the otolith edge (Fig. 2) were recorded using TPSdig software (available
139 at <http://life.bio.sunysb.edu/morph/>; Rohlf, 2007). The width of the increments was
140 computed simultaneously for all individuals from these coordinates using a Microsoft
141 Excel macro. In order to avoid uncertainties of assigning a year fraction to the width
142 defined by the last increment and the total otolith size, only full annual increments were
143 considered to fit individual growth trajectories.

144 The additional second sub-sample mentioned above was composed of 2,462
145 individuals caught at several sites in the south of Majorca Island during three sampling
146 years (2006-2008). The sampling methods include hook-and-line fishing with a monthly
147 periodicity and a set of individuals caught with small trawl gear to improve the sample
148 size of younger classes. The total fish length (± 1 mm) and the sampling date were

149 recorded for each individual caught. The additional purpose of the second sub-sample,
150 as well as improving the regression between fish and otolith size, was the validation of
151 the aging method, i.e., the evaluation of the periodicity of annuli formation. The two
152 validation methods used here assume that the formation of opaque increments (faster
153 growth) begins (roughly) simultaneously for all individuals (usually, in spring) and
154 increase in width until a new increment (the following spring) is generated. Thus, if and
155 only if the putative annual increments are annual, the monthly percentage of individuals
156 with an opaque border (or, in the second method, the averaged width of the last
157 increment after normalization by the radius of the otolith) follows, at the population
158 level, a periodic sinusoidal-like curve from spring to spring (Gordoa and Moli, 1997;
159 Pajuelo and Lorenzo, 2001; Morales-Nin and Panfili, 2005).

160 Sagittal otoliths were used for age determination and for measuring otolith
161 radius and increment widths in both sub-samples described above. Whole otoliths were
162 immersed in a glycerine-ethanol (1:1) solution to improve the visualization of annual
163 increments. Each otolith was examined twice by a single reader, with an interval of 2-3
164 months between readings. When the two readings of the same otolith differed, a third
165 reading was conducted. If this third reading was inconclusive, the otolith was discarded
166 and considered unreadable.

167 Regarding the sex-determination of each individual (i.e., *D. annularis* did not
168 show any sexual dimorphism) gonads were removed from all individuals and
169 immediately fixed in 3.6% buffered formalin. A middle portion of the fixed gonads was
170 extracted, dehydrated, embedded in paraffin, sectioned at 3 μ m and stained with
171 hematoxylin-eosin for microscopic analysis using a Leica DM RE (Digital Microscope
172 series RE). Consistent with the point of view of rudimentary hermaphrodites, also called

173 “late” gonochorism (Buxton and Garrat, 1990), fish were considered male when
174 functional testes were found and female when functional ovaries were present.

175 **Individual growth model**

176 The back-calculated length-at-age data obtained from the otoliths were fitted to a
177 non-linear mixed effects model adapted to longitudinal data (Pilling et al., 2002; Helser
178 and Lai, 2004; Helser et al., 2007; Zhang et al., 2009). For these purposes, the response
179 variable y_{ij} consisted of the distances from the nucleus to the j annual increment, where j
180 = 1 to t full annual increments per otolith, and $i = 1$ to N otoliths (or fish). Among
181 different possible non-linear models to fit individual growth trajectories, most of the
182 recently published analyses use the von Bertalanffy growth model (VBGM; Jones,
183 2000; Pilling et al., 2002; Helser and Lai, 2004; Helser et al., 2007; Edeline, 2007;
184 Zhang et al., 2009). This model is based on three parameters: t_0 , a growth rate (k , which
185 is constant throughout the lifespan of the individual) and an asymptotic length (L_∞). The
186 conventional form of this model is:

187

$$188 \quad y_{ij} = L_{\infty i} * (1 - \exp(-k_i * (t_j - t_{0i}))) + \epsilon_{ij}, \text{ where } i = 1 \text{ to } N \text{ (fish) and } j = 1 \text{ to } t \text{ (years)}$$

189

190 where y_{ij} is the size of the fish i at the age j , $L_{\infty i}$ is the asymptotic size at infinite
191 age, k_i is the growth rate, t_{0i} is a correction term allowing that the fish i has some
192 specific size at time = zero, and ϵ is a normally distributed error.

193 Charnov (2008) suggested that reproductive effort should negatively affect
194 growth rate. The hypothesized differences in growth rates between juvenile and mature
195 individuals are described by the so-called biphasic growth curves (Quince et al., 2008a;
196 Quince et al., 2008b). This model is intended to correct for the absence of energetic
197 costs linked to reproduction before sexual maturation (or the small energetic cost during

198 the first few years after maturation). Here, we propose a generalization of the
 199 conventional three-parameter VBGM model that allows for a change in the growth rate
 200 at a specific moment t_j of the life span of an individual of *D. annularis*. This alternative
 201 growth model based on five parameters is:

202

$$203 \quad y_{ij} = L_{\infty i} * (1 - \exp(-k_{0i} * (t_j - t_{0i}))) + \varepsilon_{ij}, \quad \text{for } t_j < t_1$$

$$204 \quad y_{ij} = L_{\infty i} * (1 - \exp(-k_{0i} * (t_{1i} - t_{0i}) - k_{1i} * (t_j - t_{1i}))) + \varepsilon_{ij}, \quad \text{for } t_j > t_1$$

205

206 where k_{0i} and k_{1i} are the growth rates before and after the moment of the change
 207 (t_{1i}). The full model is fully detailed in Appendix 1.

208 The parameters of these two growth models were determined for each individual
 209 using a Bayesian approach. Bayesian inference, although it is not free of technical
 210 problems, has recently become popular in improving the fit of the individual growth
 211 trajectories of fishes (Pilling et al., 2002; Helser and Lai, 2004; Helser et al., 2007;
 212 Zhang et al., 2009). This inference method emphasizes the inclusion of a priori
 213 information. A convenient algorithm (Markov Chains Monte Carlo; MCMC) moves
 214 iteratively around the values of the parameters that best fit the data. The distributions of
 215 these iterations directly give the probability distributions of the parameters. We adopted
 216 specific strategies to improve the convergence of MCMC chains. First, multi-normal
 217 distributions of the parameters (as suggested by Pilling et al., 2002; Helser and Lai,
 218 2004; Helser et al., 2007) were discarded because this approach implied severe
 219 convergence problems. Thus, independent normal distributions of each one of the
 220 parameters were assumed as priors. Simulations done using data generated by correlated
 221 growth parameters (and using between-parameter correlation values similar to those
 222 obtained by Pilling et al. (2002) showed that the use of independent distributions (three

223 or five, depending on the VBGM) assures a very good recovery of the actual values of
224 the parameters. This strategy allowed us to simplify the model and explore a posteriori
225 correlations between parameters. Second, t_0 was considered fixed (i.e., all individuals
226 from the population have the same value). This strategy was proposed by Zhang et al.
227 (2007) and greatly alleviates convergence problems because it considerably reduces the
228 number of parameters to be estimated. Again, the outcome of this approximation was
229 accepted because simulated data with a variability level similar to that reported by
230 Pilling et al. (2002) showed that it has a very small impact on all the other parameters
231 estimated.

232 We used semi-informative priors. They were based on the reasoning that all
233 individuals of the same sex were sampled from a common normal distribution (Mean=0,
234 tolerance (1/square root of sd) = 10^{-6}). However, normal distributions were constrained
235 to be within the interval of 2 to 6 mm for L_∞ (length on the otolith scale), and from 0 to
236 1 for the growth rates (ks). These values were based on the previous literature reported
237 for this species (Gordoa and Moli, 1997; Pajuelo and Lorenzo, 2001; Matic-Skoko et
238 al., 2007). The parameter t_1 (change in the growth rate) was not constrained at all (flat
239 prior). Priors for between-sex differences were assumed to be uniform distributions: 2 to
240 6 mm (length on the otolith scale), 0 to 7, and 0 to 0.4 were used for L_∞ , t_1 and growth
241 rates, respectively. Variance was assumed to be invariant to age and gamma-distributed
242 (flat prior). In all cases, a posteriori distributions were much narrower than a priori
243 distributions.

244 The units for L_∞ are in mm (distance from the otolith center to the border,
245 following the growth path). However, in order to make an easier interpretation, in some
246 graphs, the scale was translated to fish size (TL) using the linear relationship between
247 otolith size and fish size.

248 Three MCMC chains were run using randomly chosen initial values for each
249 individual (within a reasonable interval), and convergence criteria were checked by
250 visual inspection of the sample history for each parameter estimated. A different
251 number of iterations depending of the VBGM (Beg = 1200 in the 3-p based and Beg =
252 2500 in the 5-p based) were not considered prior to convergence of the MCMCs.
253 Autocorrelation was also checked, and thinning (in the case of VBGM 3-p, no thinning
254 was needed, and in the VBGM 5-p, only one out of five consecutive values was kept)
255 was adopted to assure independence of values within each chain. The number of
256 iterations was selected for each run to obtain at least 2700 valid values for the 3-p
257 VBGM and 1600 for the 5-p VBGM after convergence and thinning. Runs of each
258 model lasted approximately 3000 s and 9900 s, respectively. Models were implemented
259 using the library BRugs of the R-package (<http://www.r-project.org/>) known as
260 OpenBugs (<http://mathstat.helsinki.fi/openbugs/>).

261 **Results**

262 **Age and size distributions**

263 The annuli from the sagittal otolith of *Diplodus annularis* were easily and
264 clearly identifiable (Fig. 2). From the first sub-sample (i.e., the individuals for back-
265 calculating length-at-age; n= 423), 372 (87.9%) were successfully aged and analyzed.
266 With respect to the second sub-sample (n = 2,462), a total of 2,242 (91.1%) otoliths
267 were successfully aged. The sex ratio of the first sub-sample was 1.17 females per male.
268 The total length of the females varied from 92 mm to 209 mm with an average (\pm S.D.)
269 of 147.8 (\pm 21.3) mm. Males varied from 84 mm to 193 mm with an average of 138.6
270 (\pm 20.5) mm. The ages varied from 0 to 9 years with an average of 3.83 (\pm 1.6) years for
271 the females, and from 0 to 8 years and an average of 3.31 (\pm 1.5) years for the males.
272 Figure 3 shows the distribution of observed values by the classes of age and size

273 structure of males and females. Size- and age-frequency distributions for each sex (Fig.
274 3) are clearly in agreement with the rudimentary hermaphrodite reproductive strategy
275 hypothesis.

276 **Aging validation**

277 The marginal increment evolution confirmed that *D. annularis* follows a
278 periodic sinusoidal-like curve from spring to spring. Thus, annual periodicity of putative
279 annual increments is assumed for this species. The annual variations in the percentage
280 of translucent last increments for different ages are shown in Fig. 4 and the marginal
281 increment widths are shown in Fig. 5. Individuals sampled with translucent marginal
282 increment rose 100% during the winter months, coinciding with the slow growth
283 season. At the beginning of March, the number of individuals with opaque marginal
284 increment increased (Fig. 4). During May, June and July percentages of individuals with
285 opaque marginal increment raised up the 100% coinciding with the warm season (Fig.
286 4). Results also showed how young individuals presented a shorter opaque marginal
287 increment than older individuals (i.e., 2-3 vs. 4-5 years old, Fig. 4). At the end of
288 summer (i.e., from August to September), the percentage of otoliths with opaque last
289 increments decreased and the translucent last increments increased again 100% in the
290 winter (Fig. 4). This pattern was confirmed by studying the averaged marginal
291 increment ratio. This ratio was small in summer and increased until the initiation of a
292 new opaque band (Fig. 5). During the period of May to March (i.e., when initializing
293 the opaque band), between-individual variability was high, since individuals finalizing
294 the translucent (i.e., with large marginal increments) band and initiating the opaque
295 band (i.e., with short marginal increments) were sampled together (Fig. 5).

296 **Individual growth patterns**

297 The linear regression between the fish total length and the otolith size showed a
298 very good relationship (Fig. 6, $r^2 = 0.88$), suggesting that otoliths can be used as a
299 reliable proxy of somatic size in order to reconstruct ontogenetic growth trajectories.
300 Preliminary runs to fit the individual growth trajectories of the 372 individuals from the
301 first sub-sample showed poor performance of the Bayesian approach, due to the fact that
302 young individuals (1 or 2 years old) were fit with difficulties. Thus, estimation of
303 individual growth parameters was reduced to 166 females and 141 males 3 years old or
304 older. The results obtained after fitting individuals 4 years old or older were
305 qualitatively the same as those obtained with 3 years and older individuals. Therefore,
306 hereafter, only the results corresponding to the analyses of 3 years old and older
307 individuals were used to describe the individual growth pattern and its variability.

308 The fit of the length-at-age data in a non-linear hierarchical mixed effects model
309 based on the conventional three-parameter VBGM (L_∞ , t_0 and k) did not provide a good
310 fit of the data (Fig. 7). This model showed a systematic error in the prediction of the fast
311 growth experienced during the first two-three years of the lifespan of *D. annularis*.
312 Related to this, conventional VBGM also implies an important overestimation of the old
313 ages. As a consequence, L_∞ was also dramatically underestimated (Table 1 and Fig. 8).
314 In fact, old individuals displayed an estimation of their L_∞ lower than the observed total
315 length at the moment of catch. Observed and predicted sizes for a specific individual are
316 shown in Fig. 7. The distribution of the residuals proved that this bias was systematic
317 for most of the individuals and suggested that a change in the growth when individuals
318 were around 2 or 3 years old could exist (Fig. 7). This fact motivated the use of an
319 alternative version of the VBGM that allows for one change of growth rate. The five-
320 parameter version better accommodated the fast growth during the younger years and
321 provided better estimations of size at old ages (after “ t_1 ”; see M&M). The residuals of

322 this alternative VBGM model did not show severe age-related biases, and they were
323 closer to zero (Fig. 7). Moreover, the results of the estimation of the L_{∞} were more
324 robust and logical from the biological standpoint (Table 1 and Fig. 8). These two facts
325 support the use of only the second model in the next section for describing individual
326 and sex-related variability.

327 **Individual and between-sex growth variability**

328 The mean, standard deviation and Bayesian credibility interval obtained for
329 males and females are shown in Table 1. The 95% credibility interval for L_{∞} for females
330 varied between 211.3 and 232.3 mm, with a mean of 219.3 mm. Males varied from
331 208.1 to 213.9 mm, with a mean of 210.2 mm (Table 1 and Fig. 8). The small overlap
332 between these intervals indicated that the asymptotic length is larger for females than
333 for males (9.1 mm, Fig. 9).

334 The Bayesian means of t_0 were similar for both sexes, with a large overlap of
335 the Bayesian credibility intervals (Table 1). The estimate was -0.17 for females and -
336 0.16 for the males. Regarding the parameter t_1 (i.e., the time where the change in the
337 growth rate was produced), the 95% credibility interval varied from 1.2 years to 3.2
338 years for the females and from 1.2 years to 2.9 years for the males. The means were 2.2
339 years for the females and 2.1 years for the males (i.e., females matured slightly later
340 than males, but credibility intervals overlapped considerably).

341 The individual means of the initial growth rate (k_0) ranged from 0.21 year⁻¹ to
342 0.38 year⁻¹ for females and from 0.2 year⁻¹ to 0.39 year⁻¹ for males. Note the large
343 variability of this parameter. Nevertheless, mean k_0 s are very close for males and
344 females, and Bayesian credibility intervals largely overlap (Table 1 and Fig. 9).
345 Regarding k_1 , all estimated individual values were lower than k_0 , thus showing a
346 decrease in the growth rate at a specific moment of the life span of *D. annularis* (at t_1).

347 The individual means ranged from 0.09 year⁻¹ to 0.19 year⁻¹ for females and from 0.09
348 year⁻¹ to 0.28 year⁻¹ for males. Females presented a lower mean k_1 than males (Fig. 9).
349 Therefore, after the change in the growth rate, females grow more slowly than males.

350 Correlations between the growth parameters were low in most cases. First, the
351 growth rates (i.e., k_0 and k_1) did not show any tendency for either females ($r^2 = 0.02$) or
352 males ($r^2 = 0.09$). Therefore, the growth after the change in the growth rate was not
353 dependent on the initial rate. The time of change in the growth rate seemed independent
354 of the initial growth rate, both for females ($r^2 = 0.03$) and males ($r^2 = 0.14$). Finally, it
355 has been suggested that the relationship between L_∞ and growth rate should reflect a
356 trade-off between somatic growth and reproduction. Consequently, there is a general
357 assumption that these parameters should be negatively correlated at the individual level.
358 Here, L_∞ and growth rates presented a clear relationship, both for k_0 (females, $r^2 = 0.33$
359 and males, $r^2 = 0.33$; Fig. 10) and k_1 (females, $r^2 = 0.31$ and males, $r^2 = 0.11$; Fig. 10).
360 However, in contrast with the cases reported based on conventional VBGM, the slopes
361 of the regressions were positive in all cases (Fig. 10). Thus, individuals with fast growth
362 (before and after the change in the growth rate) become the individuals with larger L_∞ .

363 **Discussion**

364 Growth is one of the most important biological characteristics when coping with
365 population dynamics and management issues of exploited fishes. However, the most
366 common approach used to describe population growth is as an average of a common
367 von Bertalanffy growth model, thus ignoring individual variability. Recent trends in
368 fishery science highlight the importance of fitting individual growth curves from length-
369 at-age data (Wang and Ellis, 1998; Troynicov and Walker, 1999; Pilling et al., 2002).
370 Description of individual variability is more easily provided using Bayesian inference.
371 This novel approach allows for obtaining robust results, even when short temporal

372 series are available (i.e., short lifespan). Indeed, this kind of inference has recently
373 revealed the high individual variability exhibited by the individuals from some
374 populations and how it impacts population dynamics (Wang and Ellis, 1998; Helser and
375 Lai, 2004; Helser et al., 2007).

376 In the present study, we describe the individual growth pattern of a small Sparid,
377 *Diplodus annularis*. This species has low commercial value, but it is an important
378 target species for local recreational anglers. As recommended by Pilling et al. (2002),
379 we fitted the individual trajectories using a non-linear random effects model. This type
380 of model is commonly used for the estimation of individual growth parameters and
381 seems to behave better (Pilling et al., 2002; Helser and Lai, 2004; Helser et al., 2007).
382 The reason for this enhanced behavior is that these types of models incorporate each
383 individual data set but combine these individual data with the population average
384 (Pilling et al., 2002).

385 The growth of fishes has historically been described using the von Bertalanffy
386 curve based on three parameters, namely the t_0 , the growth rate (k), which is assumed to
387 be constant throughout the life span of the fish, and an asymptotic length (L_∞). This
388 model has usually been applied at the whole population level (i.e., a conventional one
389 fish-one data approach) and, most recently, at the individual level (i.e., individual
390 growth trajectories). The results for the species analyzed here show poor success of this
391 model to fit and predict the individual back-calculated data. Previous research on the
392 growth of this species at the population level (i.e. one fish one datum) anticipated that
393 the conventional von Bertalanffy model would not fit the growth of this species well
394 (Gordoa and Moli, 1997). This failure may be associated with the fast growth during the
395 first 1-2 years of life. Specifically, residuals (observed minus predicted size) showed a
396 systematic bias depending on age. Consequently, the conventional three-parameter

397 model resulted in a dramatic underestimation of the L_{∞} . In fact, most of the large and
398 old fish sampled showed a Bayesian mean of the L_{∞} lower than the size at capture. This
399 bias has been already noted at the population level (Gordoa and Moli, 1997). Thus, the
400 values obtained for this parameter were unrealistic from the biological standpoint. The
401 main cause of this failure seems to be the assumption that the growth rate (k) is constant
402 during the lifespan.

403 Here, we use an alternative five-parameter growth model based on the
404 assumption that *D. annularis* changes its growth rate at some moment during the
405 lifespan. Therefore, we proposed an individual growth model based the conventional
406 von Bertalanffy curve during the first years of life (i.e., with a growth rate k_0). This
407 period is characterized by a fast growth, and fits the early ages of an individual of *D.*
408 *annularis* very well. Then, at around 2-3 years of age, fish experience a decrease in
409 growth with a smaller growth rate, k_1 . This five-parameter model (t_0 , t_1 , k_0 , k_1 , and L_{∞})
410 better fits the individual growth of *D. annularis*. This model accommodated the fast
411 growth in early life stages and fitted the decrease in growth rate after the age of change
412 well. This alternative model allowed for better estimates of the parameters, with lower
413 variability, and was more realistic from the biological standpoint. In fact, the previously
414 reported values of L_{∞} estimated at the population level ranged from 203.7 mm to 239.5
415 mm (Gordoa and Moli, 1997; Pajuelo and Lorenzo, 2001; Matic-Skoko et al., 2007),
416 and the Bayesian means estimated from the conventional von Bertalanffy growth model
417 were 159.3 mm and 151.7 mm for the females and males, respectively. However, using
418 the conventional growth model, the Bayesian mean values obtained rose the 220 mm for
419 both sexes.

420 A non-constant growth rate is a relatively novel topic in the research involving
421 fish and fisheries at individual growth level. A general assumption exists that there is a

422 trade-off between the allocation of the energy required for somatic growth and
423 reproduction (Lester et al., 2004; Charnov, 2008). This is based on the assumption that
424 the growth rate of fishes (k) is proportional to the reproductive effort (Charnov, 2008).
425 Several authors proposed a “biphasic” growth curve to correct for the lack of the
426 energetic cost of reproduction after maturation (Day and Taylor, 1997; Lester et al.,
427 2004; Charnov, 2008; Quince et al., 2008a; Quince et al., 2008b). Recently, Quince et
428 al. (2008b) recommended that this kind of model should be used to fit the growth of
429 fishes that present a differential pattern related to sexual maturity.

430 In the case of *D. annularis*, the existence of a change in the growth rate at the
431 moment of sexual maturity seems to explain the individual growth pattern of this
432 species well. First, this species matures at 100 mm in females and 90 mm in males
433 (Matic-Skoko et al., 2007). Assuming that the individuals analyzed here mature at
434 similar sizes, this implies that they mature during the 2nd or 3rd year of life. This figure
435 agrees with the distribution of the Bayesian mean t_1 for the population (i.e., the age of
436 the change in the growth rate). Thus, the parameter t_1 could relate the trade-off
437 previously assumed between the somatic growth and reproduction. Consequently, the
438 individual growth pattern of this species is characterized by an allocation of the energy
439 to somatic growth during the first years of life (fast growth) and, after that, a
440 redistribution of the energy to reproduction with a cost in somatic growth, and in
441 consequence, a decrease in the growth rate.

442 Moreover, there were differences in the growth pattern between sexes. Females
443 change the growth rate slightly later than males, and females mature at larger sizes than
444 males. *D. annularis*, along with other members of the family Sparidae, is catalogued in
445 the Mediterranean area as a rudimentary hermaphrodite (Buxton and Garrat, 1990;
446 Matic-Skoko et al., 2007). This reproduction style includes an immature hermaphrodite

447 gonad prior to maturity of the individual; after that, the individual progresses to either a
448 functional female or male (Buxton and Garrat, 1990). It is reasonable to assume that the
449 growth in immature individuals of *D. annularis* (i.e., immature hermaphrodites) is
450 similar for functional females and males. Results obtained here agree with this
451 statement (i.e., k_0 from males and females are very similar). In contrast, post-maturity
452 growth was different between functional females and males, since females grow less
453 than males. This result is explained by the likely fact that energy costs associated with
454 gamete production are different between sexes (costs related with testes maturation are
455 probably negligible compared with those of ovarian maturation; (Adams et al., 1982;
456 Wootton, 1985).

457 In addition to between-sex differences, it was expected that the relationship
458 between L_∞ and growth rate at the individual level would be negative since it is
459 considered a trade-off between somatic growth and reproduction. In fact, Pilling et al.
460 (2002) reported the first reliable confirmation for this negative correlation, which was
461 recently supported by Helser et al. (2007). However, when we fitted the alternative five-
462 parameter von Bertalanffy model, the relationship between growth rates (k_0 and k_1) and
463 the asymptotic length (L_∞) became positive in both sexes. Both the five-parameter
464 growth model proposed here and all biphasic growth models explicitly allow for
465 explaining the energy demand imposed by reproduction (Lester et al., 2004; Charnov,
466 2008; Quince et al., 2008a; Quince et al., 2008b). In accordance with this theoretical
467 framework, the individuals of *D. annularis* with high growth rates (both before and after
468 sexual maturation) displayed large asymptotic length since their growth is faster and the
469 demand imposed by reproduction is already explicitly included in the growth curve.
470 This assumption, although it seems biologically and ecologically sound and agrees with
471 previous research in this topic, needs further research 1) involving multiple populations

472 (i.e. increasing the range of the growth parameters), 2) increasing the spatial scale (i.e.
473 (i.e. to increase individual variability), and 3) providing qualitative descriptions of the
474 reproductive potential (e.g., fecundity) at the individual level.

475 Other interesting topic for further research is disentangling the seasonal patterns
476 of the individual growth. Fishes displays seasonal oscillations since they grow faster in
477 warm seasons. The first approaches to the seasonal growth were published by Ursin,
478 1963. After that, number of authors have been published different kind of models to
479 coping with the seasonal growth (e.g. Pitcher and Macdonald, 1973; Cloern and
480 Nichols, 1978; Pauly et al., 1992). Thus, further research in the individual growth of this
481 species must emphasize in 1) determinate the moment of the change in the growth rate
482 inside the year and its variability and 2) include a sinusoidal curve in the biphasic
483 growth model adopted in the present Bayesian approach allowing seasonal oscillation.

484 In conclusion, the approach adopted here allows for the accurate description of
485 the individual growth patterns of *D. annularis* on several scales. Combining the
486 Bayesian approach, non-linear mixed effects models, and the biphasic growth pattern
487 revealed that this species showed a change in the growth rate during its lifespan. The
488 existence of biphasic growth is well explained by assuming differential allocation of the
489 energy to either somatic growth or reproduction. This model has been successfully
490 implemented for this short lifespan species and could be used to disentangling the
491 individual growth patterns for other coastal species and to improve the knowledge for
492 long live species. Moreover, we demonstrated the differences in growth between
493 females and males in a rudimentary hermaphrodite never previously described. The
494 knowledge of individual variation is the input of, for example, individual-based models
495 (Martinez-Garmendia, 1998) that are intended to elucidate the biological significance
496 and the expected outputs of growth variability on population dynamics. The ultimate

497 goal for explicitly incorporating growth knowledge into management models must be to
498 establish sustainable exploitation levels of this recreational target species.

499 **Acknowledges**

500 The authors would like to thank the people from the National Park of Cabrera
501 Archipelago for their cooperation. Appreciation is extended to the researcher involved
502 in the experimental angling sessions and sampling procedures. Especially thanks for
503 A.M. Grau (DG Pesca) and Dr. S. Balle (IMEDEA) for their helpful suggestions. The
504 Figure 1 was provided by D. March. This study was founded by the research project
505 ROQUER (CTM2005-00283) funded by Ministerio de Educación y Ciencia of the
506 Spanish Government. Finally, we would like to thank two anonymous reviewers for
507 their useful comments. The first author was supported by a FPI fellowship (MICINN).

508 **References**

- 509 Adams, S.M., Malean, R.B., Parrota, J.A., 1982. Energy partitioning in Largemouth
510 bass under conditions of seasonally fluctuating prey availability. *Trans. Am.*
511 *Fish. Soc.* 111, 549-558.
- 512 Alós, J., Palmer, M., Grau, A.M., Deudero, S., 2008. Effects of hook size and barbless
513 hooks on hooking injury, catch per unit effort, and fish size in a mixed-species
514 recreational fishery in the western Mediterranean Sea. *Ices J. Mar. Sci.* 65, 899-
515 905.
- 516 Bauchot, M.L., 1987. Sparidae. In: Fischer W., Bauchot, M.L., Schneider, M. (Eds.),
517 Fiches FAO d'Indentification des espèces pour les Besoins de la Pêche (Revision
518 1), Méditerranée et Mer Noire. Zones de pechê 37, Vol. II (Vertébrés). FAO-
519 CEE, Rome, pp. 761-1530.
- 520 Beverton, R.J., Holt, S.J., 1957. On the dynamics of exploited fish populations. *Fish.*
521 *Invest. London Ser.* 2, 533 pp.

522 Buxton, C.D., Garrat, P.A., 1990. Alternative reproductive styles in Seabreams (Pisces,
523 Sparidae). Environ. Biol. Fishes 28, 113-124.

524 Charnov, E.L., 2005. Reproductive effort is inversely proportional to average adult life
525 span. Evol. Ecol. Res. 7, 1221-1222.

526 Charnov, E.L., 2008. Fish growth: Bertalanffy k is proportional to reproductive effort.
527 Environ. Biol. Fishes 83, 185-187.

528 Cloern, J.E., Nichols, F.H., 1978. A von Bertalanffy growth model with a seasonally
529 varying coefficient. J. Fish. Res. Board Can. 35, 1479-1482.

530 Cooke, S.J., Cowx, I.G., 2006. Contrasting recreational and commercial fishing:
531 Searching for common issues to promote unified conservation of fisheries
532 resources and aquatic environments. Biol. Conserv. 128, 93-108.

533 Day, T., Taylor, P.D., 1997. Von Bertalanffy's growth equation should not be used to
534 model age and size at maturity. Am. Nat. 149, 381-393.

535 Edeline, E., 2007. Adaptive phenotypic plasticity of eel diadromy. Mar. Ecol. Prog. Ser.
536 341, 229-232.

537 Gordo, A., Moli, B., 1997. Age and growth of the sparids *Diplodus vulgaris*, *D. sargus*
538 and *D. annularis* in adult populations and the differences in their juvenile
539 growth patterns in the north-western Mediterranean Sea. Fish. Res. 33, 123-129.

540 Haddon, M., 2001. Modelling and quantitative methods in fisheries. Chapman &
541 Hall/CRC, Washington, D.C., 406 pp.

542 Helser, T.E., Lai, H.L., 2004. A Bayesian hierarchical meta-analysis of fish growth:
543 with an example for North American largemouth bass, *Micropterus salmoides*.
544 Ecol. Model. 178, 399-416.

545 Helser, T.E., Stewart, I.J., Lai, H.L., 2007. A Bayesian hierarchical meta-analysis of
546 growth for the genus *Sebastes* in the eastern Pacific Ocean. *Can. J. Fish. Aquat.*
547 *Sci.* 64, 470-485.

548 Jackson, J.B.C., Kirby, M.X., Berger, W.H., Bjorndal, K.A., Botsford, L.W., Bourque,
549 B.J., Bradbury, R.H., Cooke, R., Erlandson, J., Estes, J.A., Hughes, T.P.,
550 Kidwell, S., Lange, C.B., Lenizan, H.S., Pandolfi, J.M., Peterson, C.H., Steneck,
551 R.S., Tegner, M.J., Warner, R.R., 2001. Historical overfishing and the recent
552 collapse of coastal ecosystems. *Science* 293, 629-638.

553 Jones, C.M., 2000. Fitting growth curves to retrospective size-at-age data. *Fish. Res.* 46,
554 123-129.

555 Lester, N.P., Shuter, B.J., Abrams, P.A., 2004. Interpreting the von Bertalanffy model
556 of somatic growth in fishes: the cost of reproduction. *Proc. R. Soc. London Ser.*
557 *Biol. Sci.* 271, 1625-1631.

558 Lewin, W.C., Arlinghaus, R., Mehner, T., 2006. Documented and potential biological
559 impacts of recreational fishing: Insights for management and conservation. *Rev.*
560 *Fish. Sci.* 14, 305-367.

561 Martinez-Garmendia, J., 1998. Simulation analysis of evolutionary response of fish
562 populations to size-selective harvesting with the use of an individual-based
563 model. *Ecol. Model.* 111, 37-60.

564 Matic-Skoko, S., Kraljevic, M., Dulcic, J., Jardas, I., 2007. Age, growth, maturity,
565 mortality, and yield-per-recruit for annular sea bream (*Diplodus annularis* L.)
566 from the eastern middle Adriatic Sea. *J. Appl. Ichthyol.* 23, 152-157.

567 Morales-Nin, B., Moranta, J., Garcia, C., Tugores, M.P., Grau, A.M., Riera, F., Cerdà,
568 M., 2005. The recreational fishery off Majorca Island (western Mediterranean):

569 some implications for coastal resource management. *Ices J. Mar. Sci.* 62, 727-
570 739.

571 Morales-Nin, B., Panfili, J., 2005. Seasonality in the deep sea and tropics revisited:
572 what can otoliths tell us? *Mar. Fresh. Res.* 56, 585-598.

573 Pajuelo, J.G., Lorenzo, J.M., 2001. Biology of the annular seabream, *Diplodus*
574 *annularis* (Sparidae), in coastal waters of the Canary Islands. *J. Appl. Ichthyol.*
575 17, 121-125.

576 Pauly, D., Soriano-Bartz, M., Moreau, J., Jarre, A., 1992. A new model accounting for
577 seasonal cessation of growth in fishes. *Aust. J. Mar. Freshwat. Res.* 43, 1151-
578 1156.

579 Pauly, D., Alder, J., Bennett, E., Christensen, V., Tyedmers, P., Watson, R., 2003. The
580 future for fisheries. *Science* 302, 1359-1361.

581 Pilling, G.M., Kirkwood, G.P., Walter, S.G., 2002. An improved method for estimating
582 individual growth variability in fish, and the correlation between von Bertalanffy
583 growth parameters. *Can. J. Fish. Aquat. Sci.* 59, 424-432.

584 Pitcher, T.J., MacDonald, P.D.M., 1973. Two models for seasonal growth in fishes. *J.*
585 *Appl. Ecol.* 10, 599-606.

586 Quince, C., Abrams, P.A., Shuter, B.J., Lester, N.P., 2008a. Biphase growth in fish I:
587 Theoretical foundations. *J. Theor. Biol.* 254, 197-206.

588 Quince, C., Shuter, B.J., Abrams, P.A., Lester, N.P., 2008b. Biphase growth in fish II:
589 Empirical assessment. *J. Theor. Biol.* 254, 207-214.

590 Rohlf, F.J., 2007. *TPS Software Series*. Department of Ecology and Evolution, State
591 University of New York, Stony Brook, USA.

592 Sainsbury, K.J., 1980. Effect of individual variability on the von Bertalanffy growth
593 equation. *Can. J. Fish. Aquat. Sci.* 37, 241-247.

594 Smith, E.B., Williams, F.M., Fisher, C.R., 1997. Effects of intrapopulation variability
595 on von Bertalanffy growth parameter estimates from equal mark-recapture
596 intervals. *Can. J. Fish. Aquat. Sci.* 54, 2025-2032.

597 Troynikov, V.S., Walker, T.I., 1999. Vertebral size-at-age heterogeneity in gummy
598 shark harvested off southern Australia. *J. Fish Biol.* 54, 863–877.

599 Ursin, E., 1963. On the seasonal variation of growth rate and growth parameters in
600 Norway pout (*Gadus esmarki*) in Skagerrak. *Medd. Danm. Fisk. Havunders.* 4,
601 17-29.

602 Wang, Y.G., Ellis, N., 1998. Effect of individual variability on estimation of population
603 parameters from length-frequency data. *Can. J. Fish. Aquat. Sci.* 55, 2393-2401.

604 Watson, R., Pauly, D., 2001. Systematic distortions in world fisheries catch trends.
605 *Nature* 414, 534-536.

606 Wootton, R.J., 1985. Energetics of reproduction. In: Tyler P., Calow P. (Eds.), *Fish*
607 *energetics: new perspectives*. Croom Helm. London, pp. 231-254.

608 Zhang, Z.N., Lessard, J., Campbell, A., 2009. Use of Bayesian hierarchical models to
609 estimate northern abalone, *Haliotis kamtschatkana*, growth parameters from tag-
610 recapture data. *Fish. Res.* 95, 289-295.

611 Zhang, Z.Y., Hamagami, F., Wang, L.J., Nesselroade, J.R., Grimm, K.J., 2007.
612 Bayesian analysis of longitudinal data using growth curve models. *Int. J. Behav.*
613 *Dev.* 31, 374-383.

1 Table 1
2 Summary statistics for the population Bayesian means of the growth parameters for the
3 Cabrera Archipelago using the conventional (3 parameters based) and the alternative (5
4 parameters based) von Bertalanffy growth model. For each estimated parameter, the
5 mean, standard deviation (SD), median and, lower and upper 2.5 percentiles of the
6 posterior distribution are shown for both sexes. Means of L_{∞} are expressed in otolith
7 scale and in total length (in brackets) in mm, k , k_0 and k_1 as years⁻¹, and t_0 and t_1 as
8 years.

Parameters	Mean	S.D.	Bayesian credibility intervals			
			2.50%	Median	97.50%	
Conventional 3-p VBGM						
Females						
<i>Mean (L_{∞})</i>	3.33 (159.3)	0.03	3.27	3.33	3.39	
<i>Mean (t_0)</i>	-0.12	0.02	-0.16	-0.12	-0.08	
<i>Mean (k)</i>	0.45	0.01	0.43	0.45	0.47	
Males						
<i>Mean (L_{∞})</i>	3.19 (151.7)	0.03	3.12	3.19	3.25	
<i>Mean (t_0)</i>	-0.07	0.03	-0.12	-0.07	-0.03	
<i>Mean (k)</i>	0.47	0.01	0.44	0.47	0.49	
Alternative 5-p VBGM						
Females						
<i>Mean (L_{∞})</i>	4.46 (219.3)	0.07	4.34	4.45	4.60	
<i>Mean (t_0)</i>	-0.17	0.02	-0.20	-0.17	-0.13	
<i>Mean (t_1)</i>	2.21	0.07	2.06	2.21	2.35	
<i>Mean (k_0)</i>	0.29	0.01	0.28	0.29	0.31	
<i>Mean (k_1)</i>	0.15	0.01	0.14	0.15	0.17	
Males						
<i>Mean (L_{∞})</i>	4.29 (210.2)	0.07	4.17	4.28	4.43	
<i>Mean (t_0)</i>	-0.16	0.02	-0.20	-0.16	-0.12	
<i>Mean (t_1)</i>	2.12	0.10	1.92	2.12	2.32	
<i>Mean (k_0)</i>	0.30	0.01	0.28	0.30	0.31	
<i>Mean (k_1)</i>	0.17	0.01	0.16	0.17	0.19	

9

1 Figure captions

2 Figure 1

3 Map showing the sampling site of the first sub-sample (black star) located inside the
4 National Park of the Cabrera Archipelago, south coast of Mallorca Island (NW
5 Mediterranean). The second sub-sample of individuals was sampled at several sites in
6 the south of Majorca Island (black points) including Palma Bay, Cape of Regana and
7 the waters of Cabrera Channel.

8

9 Figure 2

10 Image of different saggital otoliths of 3 years old individuals sampled during different
11 months to view the marginal increment (MI) annual evolution; (A) January, (B) March,
12 (C.a) May with translucent MI, (C.b) May with opaque MI (i.e., 4 years old fish), (D)
13 July, (E.a) September with opaque MI, (E.b) September with translucent MI and (F)
14 November.

15

16 Figure 3

17 Frequency percentages of the observed ages and fish total length resulted from the
18 population of the National Park of the Cabrera Archipelago. Frequencies are structured
19 by sexes.

20

21 Figure 4

22 Monthly percentages of otoliths with translucent marginal increments from the
23 individuals of *Diplodus annularis* sampled. Figure shows the 2 years old (n = 241), 3
24 years old (n = 435), 4 years old Age (n = 218) and 5 years old individuals (n = 114).

25

26 Figure 5
27 Mean and standard deviation of Marginal increment ratio (MIR) for the 3 (n = 435) and
28 4 years old individuals (n = 218).

29

30 Figure 6

31 Lineal simple regression between the otolith radius (mm) and fish total length (mm).
32 The samples successfully aged from the first and second sub-samples were included in
33 the regression (n = 2614).

34

35 Figure 7

36 Individual growth trajectory for an individual of *Diplodus annularis* 8 years old
37 obtained from the observed data, from fitting the conventional three-parameter von
38 Bertalanffy growth model (VBGM) and from fitting the five-parameter VBGM.

39

40 Figure 8

41 Frequency distribution of the individual Bayesian means of the asymptotic lengths (L_{∞})
42 resulted from the VBGM based in 3 or 5 parameters. Results have been structured by
43 sexes.

44

45 Figure 9

46 Bayesian confidential intervals (lower and upper 2.5 percentiles) for the growth
47 parameters L_{∞} , k_0 , k_1 and t_1 obtained from the posterior distribution of the Bayesian
48 means for each sex.

49

50 Figure 10

51 Linear simple regression between the individuals means of the parameters L_{∞} and
52 growth rates (i.e., k_0 and k_1) for each sex. L_{∞} is represented in otolith scale (mm).

53

54

55

56

57

58

59

60

61

62

63

64

65

66

67

68

69

70

71

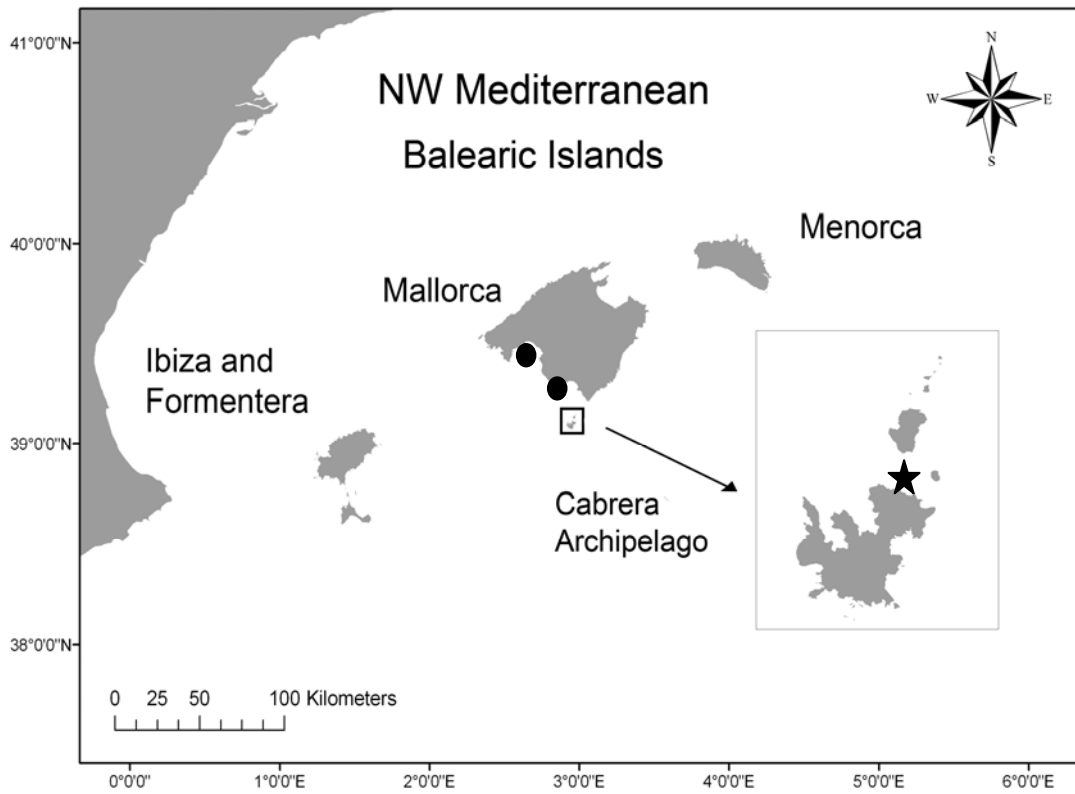
72

73

74

75

76 Figure 1



77

78

79

80

81

82

83

84

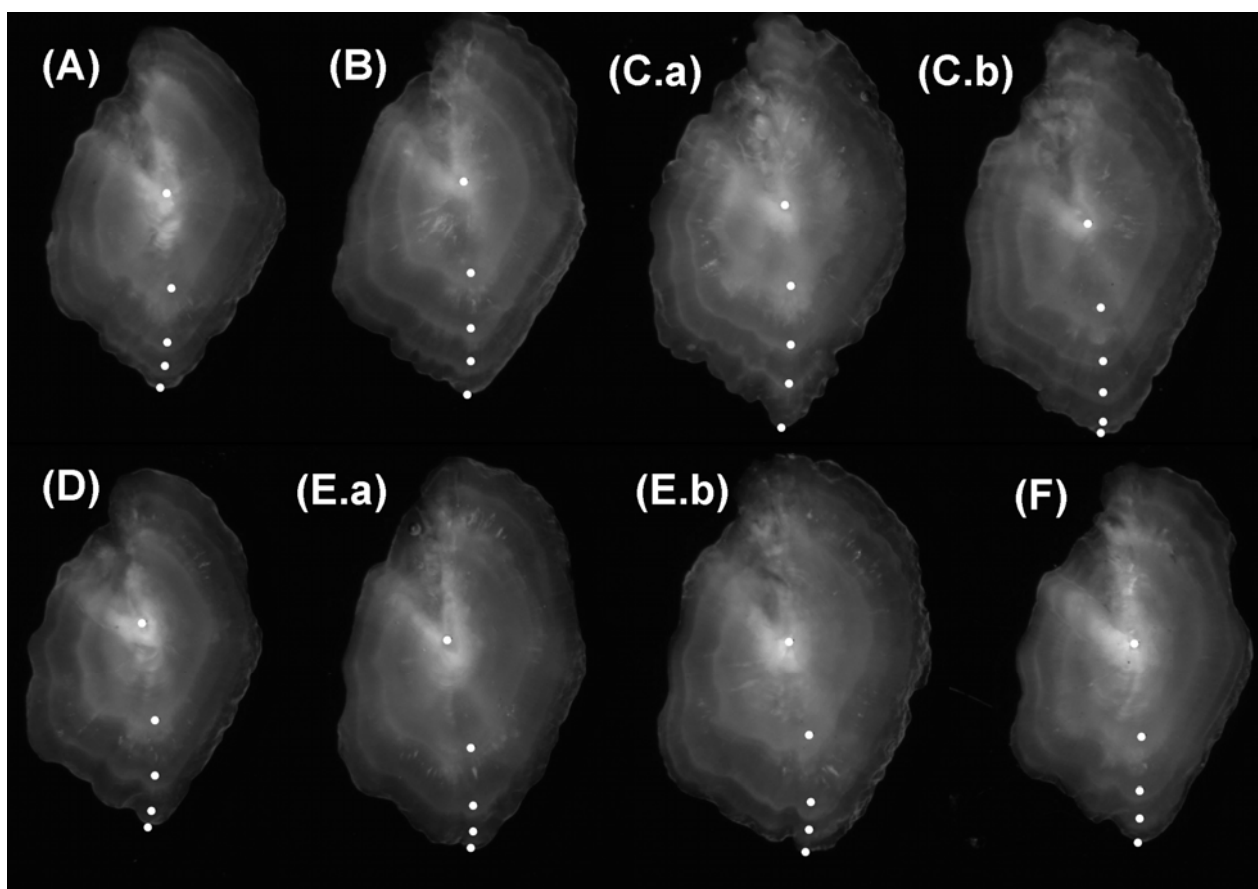
85

86

87

88

89



91

92

93

94

95

96

97

98

99

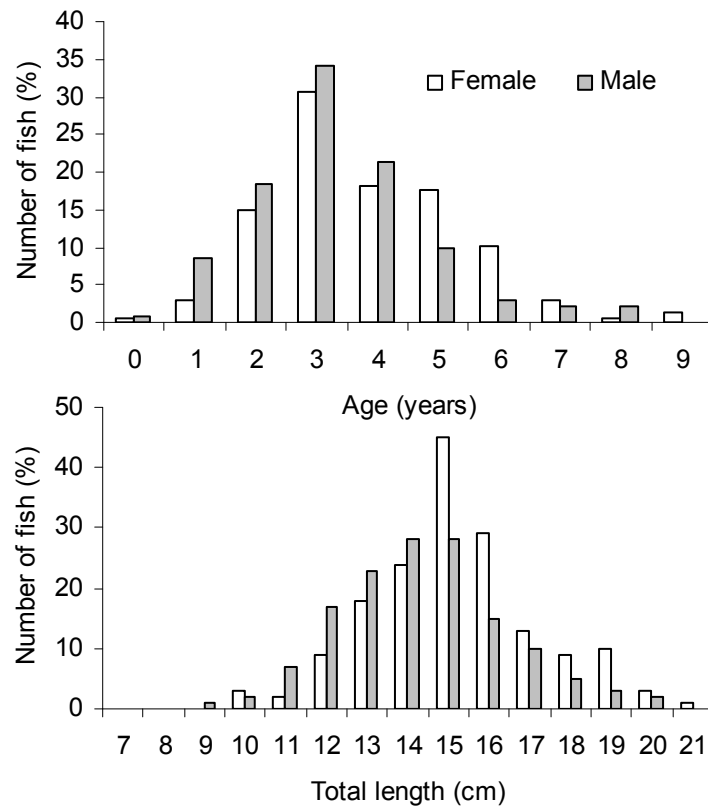
100

101

102

103

104 Figure 3



105

106

107

108

109

110

111

112

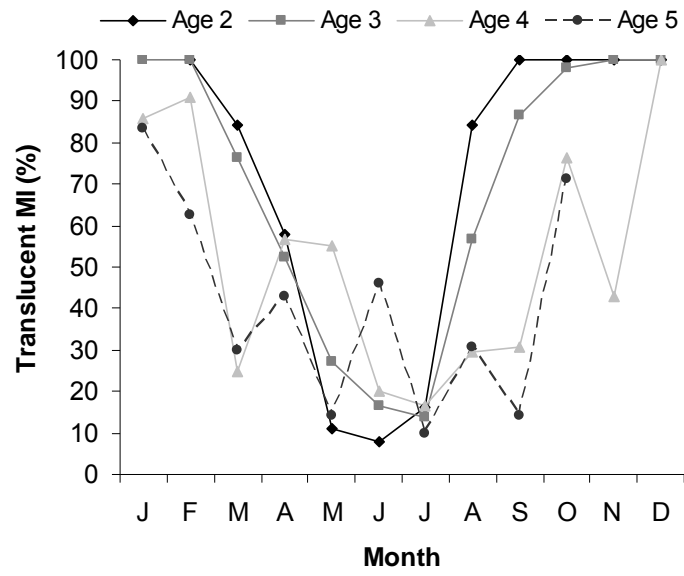
113

114

115

116

117 Figure 4



118

119

120

121

122

123

124

125

126

127

128

129

130

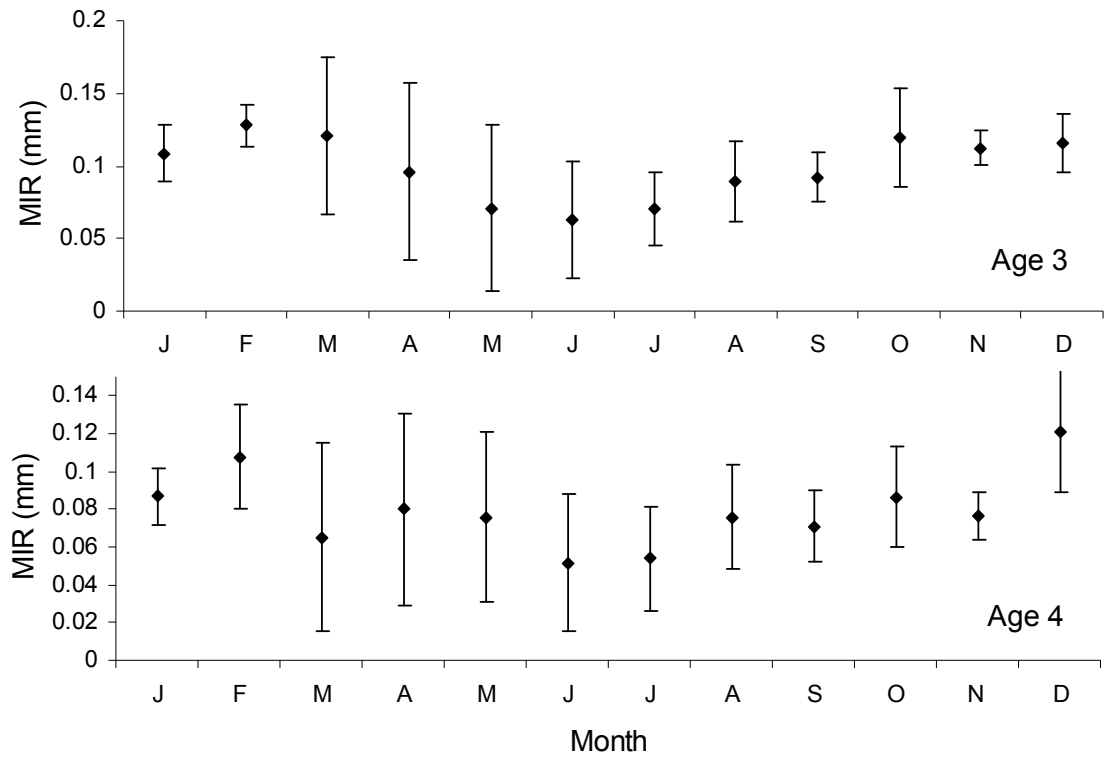
131

132

133

134

135 Figure 5



136

137

138

139

140

141

142

143

144

145

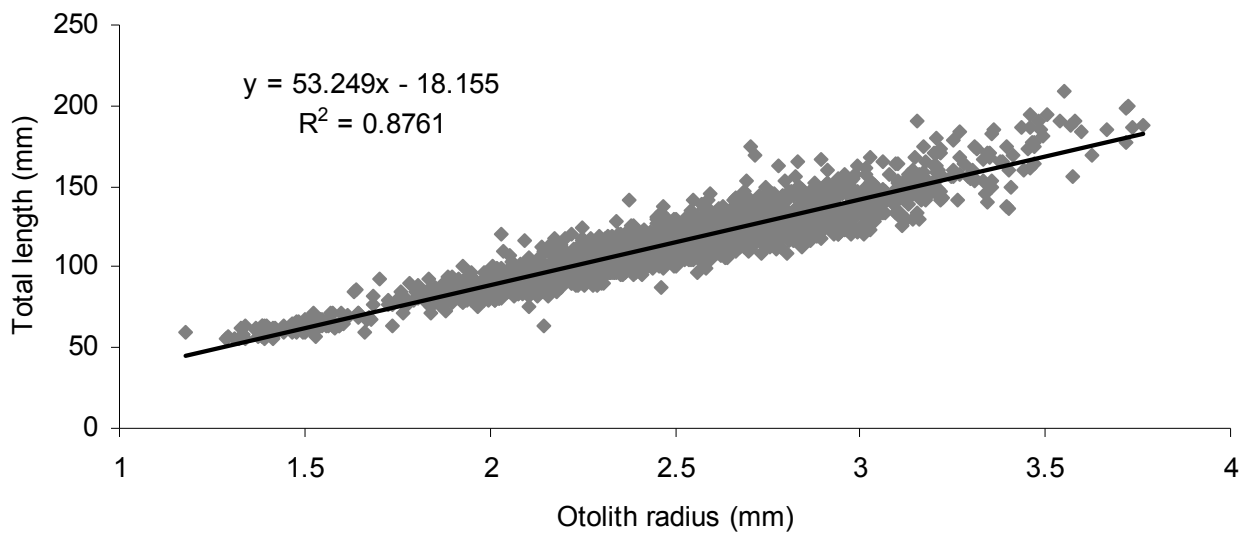
146

147

148

149

150 Figure 6



151
152

153

154

155

156

157

158

159

160

161

162

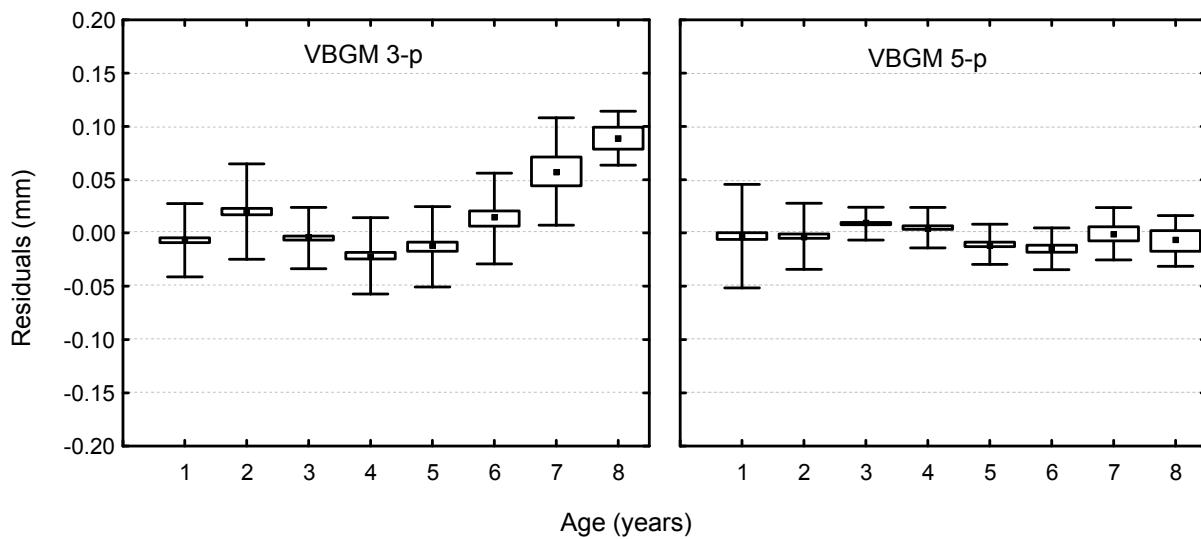
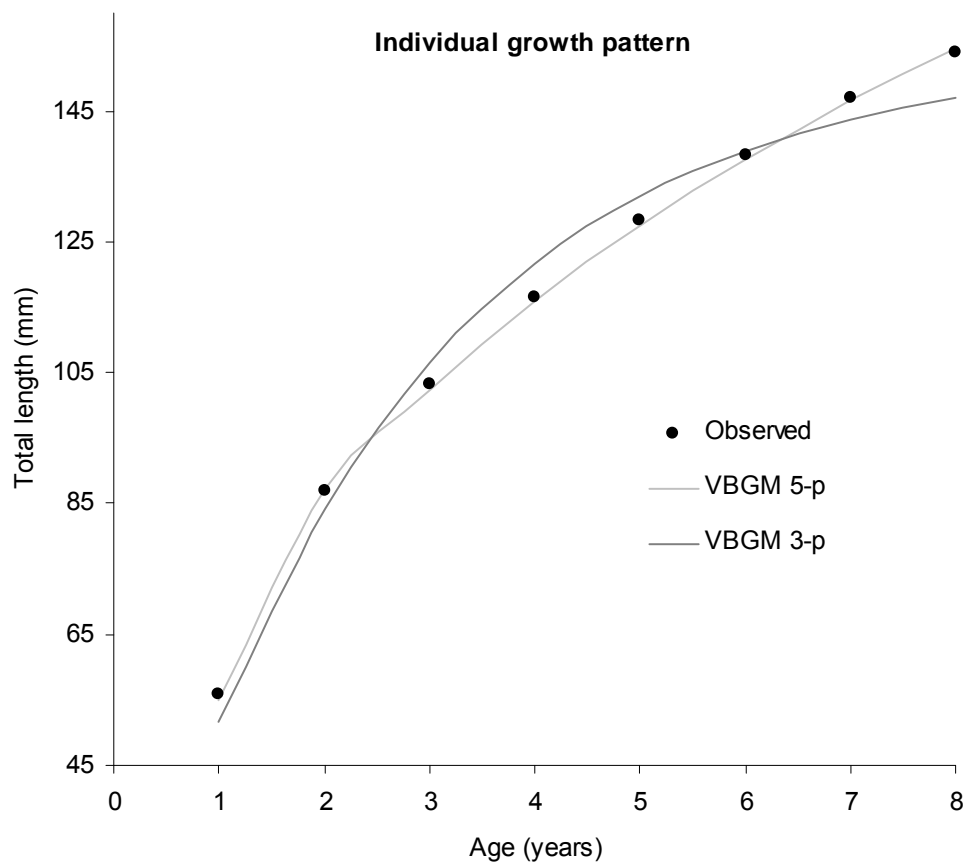
163

164

165

166

167



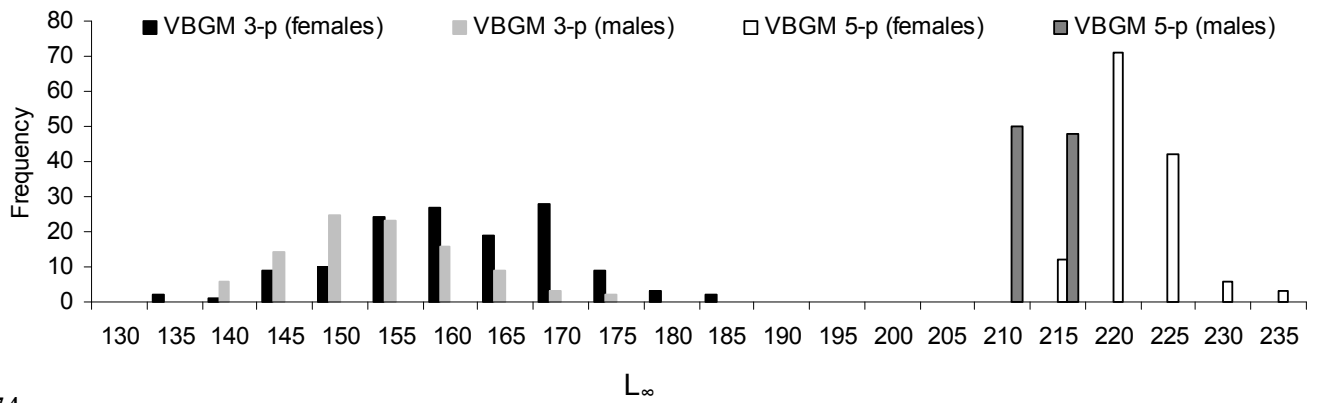
169

170

171

172

173 Figure 8



174

175

176

177

178

179

180

181

182

183

184

185

186

187

188

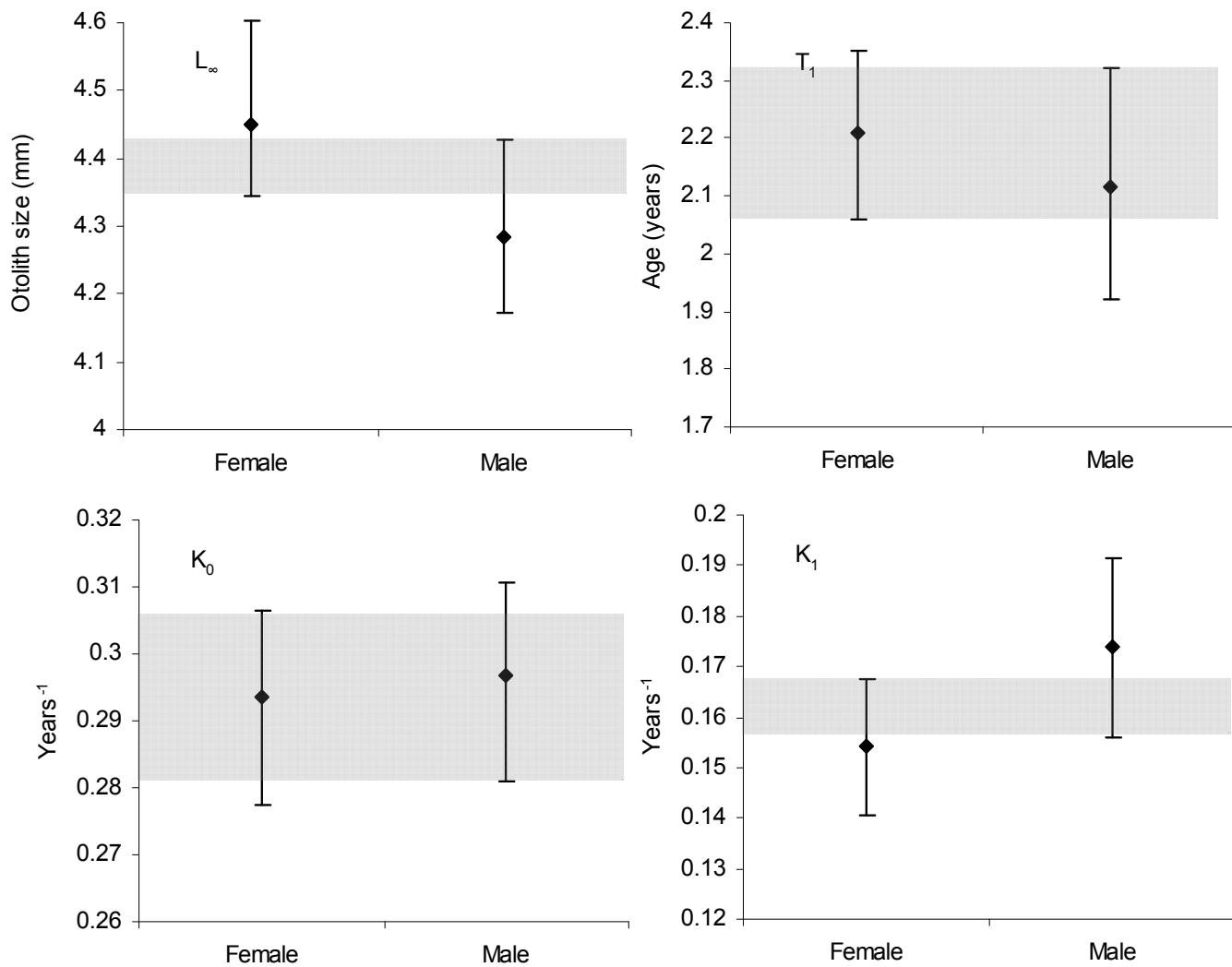
189

190

191

192

193 Figure 9



194

195

196

197

198

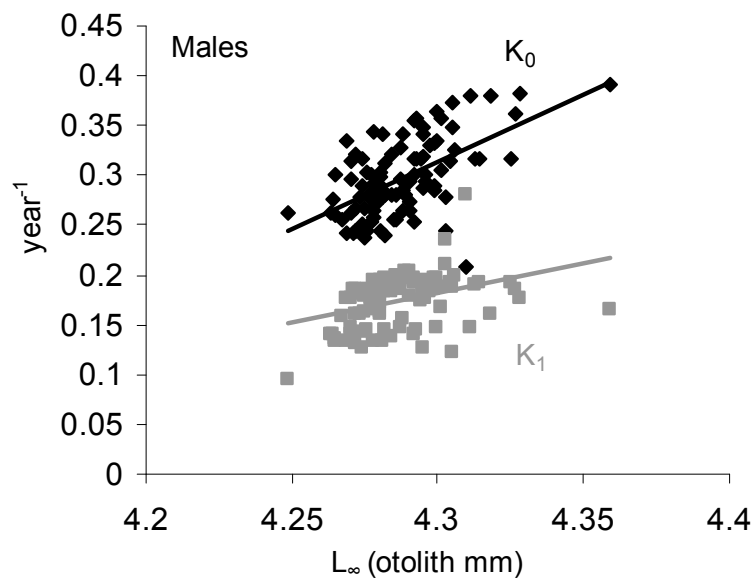
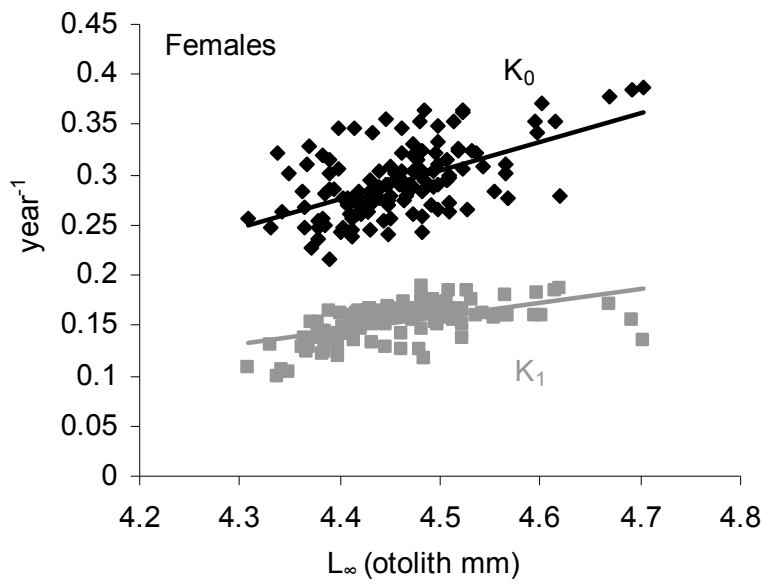
199

200

201

202

203



205

206

207

208

209

210

211

212